Automated multi-well targeting and dynamic OCT imaging of 3D in vitro cultures

Rameesa Rafi M H*[a], Ibrahim Abd El-Sadek[a,b], Rion Morishita[a], Shadil Basheer[a], Atsuko Furukawa[c], Shuichi Makita[a], Satoshi Matsusaka[c], and Yoshiaki Yasuno[a]

[a]Computational Optics Group, University of Tsukuba, Japan. [b]Department of Physics, Faculty of Science, Damietta University, Egypt. [c]Clinical Research and Regional Innovation, Institute of Medicine, University of Tsukuba, Japan

Keywords: High-throughput imaging, dynamic optical coherence tomography, spheroid, automated sample targeting.

Note: 3-page abstract can be found on the next page.

100-word abstract

We present an automated sample targeting system (ASTS) integrated with dynamic optical coherence tomography for high-throughput imaging of in vitro tumor spheroids in a 96-well plate. The system combines a Python-controlled XY motorized stage with LabVIEW-based OCT acquisition, synchronized via TCP/IP communication. The proposed system successfully performed fully automatic targeting and imaging of 15 spheroids. However, two spheroids appeared out of focus and/or the FOV. These limitations are going to be overcome in the future by adding Z-stage control and neural network-based segmentation for fine positioning. The proposed system could become a valuable tool for high-throughput anti-cancer drug screening.

250-word abstract

Three-dimensional tumor spheroids are key cancer research models, as they accurately mimic solid tumor architecture and microenvironments. These models are particularly valuable for evaluating the effectiveness of anti-cancer drugs, which necessitates monitoring spheroid structure and viability over time. For tumor spheroid assessment, the imaging modality must be label-free, 3D, and capable of high-speed and high-throughput imaging. Dynamic OCT is widely used for label-free and 3D tumor spheroid evaluation. However, its ability for throughput imaging is limited due to manual operations (i.e., manual sample targeting and focusing).

We introduce an automated sample targeting system (ASTS) integrated with DOCT for high-throughput, label-free imaging of tumor spheroids in a 96-well plate. The ASTS comprises a Python-controlled XY motorized stage and a LabVIEW-based DOCT acquisition system, coordinated via TCP/IP communication to perform fully automated, sequential imaging of preselected wells. We validated the system's performance by imaging fifteen MCF-7 breast cancer spheroids, and successfully acquired DOCT data for thirty samples without any manual control. The result exhibited characteristic dynamic signal patterns, such as lower activity in the spheroid core, consistent with the formation of necrotic regions. Two spheroids appeared out of focus and/or the field of view, which highlighted the need for fine focusing and real-time image-guided targeting.

Overall, our proposed system enables rapid, hands-free imaging of in vitro cancer models. With future extensions including automated focusing using Z-stage control, neural network-based segmentation, and fast DOCT protocols, this system could significantly accelerate drug response studies and facilitate high-throughput anti-cancer drug screening.

Automated multi-well targeting and dynamic OCT imaging of 3D in vitro cultures

Rameesa Rafi M H*[a], Ibrahim Abd El-Sadek[a,b], Rion Morishita[a], Shadil Basheer[a], Atsuko Furukawa[c], Shuichi Makita[a], Satoshi Matsusaka[c], and Yoshiaki Yasuno[a]

[a]Computational Optics Group, University of Tsukuba, Japan. [b]Department of Physics, Faculty of Science, Damietta University, Egypt. [c]Clinical Research and Regional Innovation, Institute of Medicine, University of Tsukuba, Japan

1. INTRODUCTION

Tumor spheroid is a three-dimensional(3D) culture of cancer cells that closely emulates the structure and microenvironment of in *vivo* solid tumors [1]. Therefore, tumor spheroids have been widely used for anti-cancer drug investigations [1]. The efficacy of these drugs can be assessed by their impact on the spheroid's morphology and viability.

High-throughput and label-free imaging is essential for efficient and reproducible analysis of the spheroids drug response [2–4]. Dynamic Optical Coherence tomography (OCT) is a label-free functional extension of OCT that has been widely used for tumor spheroid imaging and its drug response analysis [1]. Despite the DOCT is a label-free modality, its ability for high-throughput imaging is limited. This is because the manual and frequent sample targeting and repositioning require a long time. According to our knowledge, imaging a single spheroid in a 96-well plate requires approximately 5 minutes, including targeting. It means scanning the 96-wells requires 8 hours, which sacrifices the high throughput imaging ability and limits the temporal resolution of time-course studies.

In this study, we propose a fully automated XY-translational stage-controlled system, so-called "automated sample targeting system(ASTS)", and integrated it with a swept source OCT device for automatic targeting and DOCT imaging of tumor spheroids in a 96-well plate. The utility of the proposed system has been investigated for targeting and imaging 15 breast cancer (MCF-7) spheroids located in three different rows and five columns of a 96-well plate.

2. METHOD

2.1 Initialization and setup

Figure 1 shows the photograph of the ASTS system integrated with the DOCT microscope. The ASTS system consists of a motorized XY linear stage platform (MLS203-1, Thorlabs Inc., USA) driven by a brushless DC servo motor controller (BBD302, Thorlabs Inc., USA). A custom-written Python program is used to control the stage movement, beginning with homing (moving the motorized stage to a predefined reference position), followed by jogging (small, incremental movements for precise positioning).

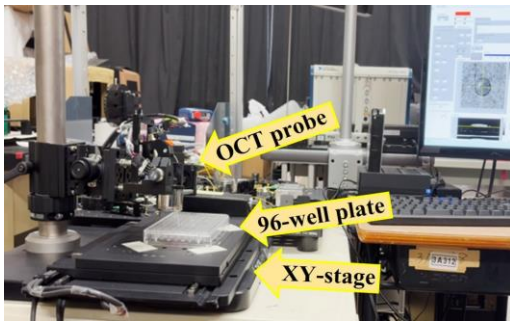

Fig 1: ASTS integrated with the DOCT

As the next step, the standard layout of a 96-well plate (see Fig. 2), 8 rows (labelled A–H) and 12 columns (numbered 1–12) is used to define the target positions for the motorized stage. In this setup, the centre of each well is treated as the target coordinate where the OCT probe is intended to move to. The wells are spaced 9 mm apart, both row-wise (vertically) and column-wise (horizontally). This means that the stage must move in 9 mm increments in the X and Y directions to switch from one well centre to the next. For example, if the top-left well (A1) is at coordinate (X_0, Y_0), then the adjacent well to the right (A2) will be at (X_0 + 9 mm, Y_0), and the one below (B1) will be at (X_0, Y_0 + 9 mm). Hence, the stage can move in a controlled manner throughout the scanning time and can efficiently target each well.

2.2 Synchronizing the stage control and automated OCT acquisition

The motorized stage, which is controlled via Python, and the OCT system, operated through LabVIEW, were integrated using a TCP/IP communication protocol of LabVIEW. This architecture ensures coordinated movement of the stage and timely image acquisition without manual intervention. In this setup, the Python script functions as the master by sending TCP signals to LabVIEW to trigger OCT image acquisition after positioning the stage at each well. LabVIEW, functioning

as the acquisition client, waits for incoming commands and performs acquisition accordingly. Once the acquisition of one well is completed, the Python program monitors and confirms the OCT raw data saving, and moves the stage to the next well for further acquisition. In this way, automated sequential imaging of the 96-well plate is achieved and fully eliminates manual interventions and ensures precise timing between jogging and acquisition.

2.3 Sample preparation and scanning protocol

The operation of ASTS is validated by imaging 15 MCF-7 spheroid samples of approximately 500 µm size. 1,000 human breast cancer cells (MCF-7 cell line) were seeded in 15 wells (as highlighted in Fig. 2) of a U-shaped bottom ultra-low attachment 96-well plate to form spheroids. After 6 days of cultivation, the 96-well plate was extracted from the cultivation environment, held on the XY translation stage, and measured using the proposed system. Before starting the acquisition, the labels of the wells containing the spheroids were predefined in the Python control program. The Python-controlled XY translation stage followed a raster well-visiting scanning [red dashed line in Fig. 2] starting from B4 (contains spheroid 1) up to D8 (contains spheroid 15) by completing the acquisition across all the wells.

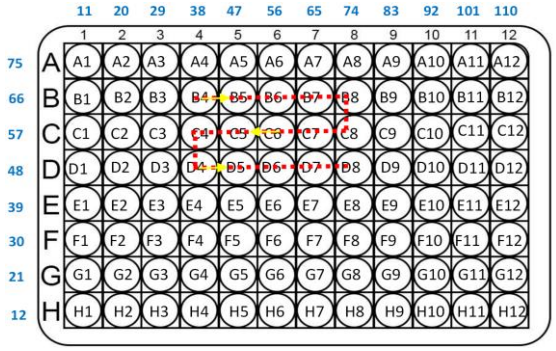

Fig 2: Schematic of a standard 96-well plate with position coordinates and highlighted the raster well-visiting pattern followed by the XY-stage

A 1.3-µm swept-source OCT device, operating at a speed of 100,000 A-lines/s, is used in this study. The objective used was LSM03 (Thorlabs), which has a focal length of 36 mm and provides an axial (in tissue) and lateral resolutions of 16.3 µm and 18.1 µm, respectively. For DOCT imaging, a lateral imaging field of 1 × 1 mm^2 was divided into 4 blocks, and each block consists of 32 B-scan locations [1]. Each block was raster scanned 32 times in 6.48 ms. Hence, at each B-scan location, 32 repeated frames were captured with an inter-frame interval of 207.36 ms. An OCT volume comprising 128 locations was captured in 26.4 seconds for each sample.

2.4. DOCT algorithms

To assess the intracellular dynamics, we used two DOCT algorithms: logarithmic-intensity variance (LIV) and OCT correlation decay speed ($OCDS_l$) [1]. The LIV is computed as the time variance of the logarithmic (dB-scaled) OCT intensity. And it is sensitive to the occupancy of the dynamic scatterers within the tissue [5]. The $OCDS_l$ is defined as the slope of the autocorrelation decay curve of the sequentially captured OCT frames at each B-scan location at a delay range of 512 pixels. $OCDS_l$ was supposed to be sensitive to a certain velocity range of the intracellular scatterers [5].

3. RESULTS

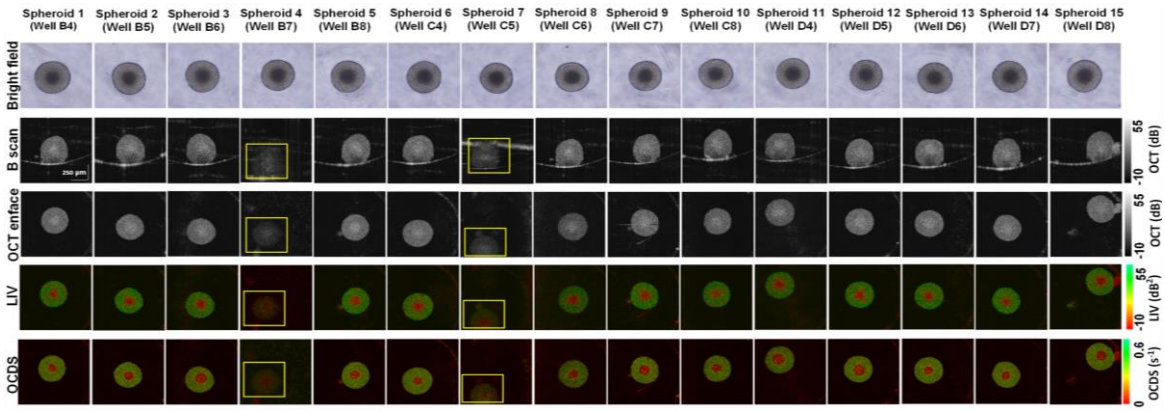

Fig 3: Automatically captured OCT and DOCT images of MCF-7 spheroid. The panel includes bright field, OCT B-scan, and enface, and the corresponding LIV and OCDS enface images of 15 MCF-7 spheroids acquired automatically. The spheroids that were out of focus or out of the field of view (FOV) are highlighted by the yellow squares.

Figure 3 shows the Bright field, OCT, and DOCT images of the 15 measured spheroids. Out of the 15 spheroids targeted, 13 were successfully imaged using the automated system. And they exhibited the well-known DOCT patterns of the spheroid. Namely, the spheroid centre exhibited reduced LIV and $OCDS_l$ signals (red) [Fig.3 (4^{th} and 5^{th} rows, respectively)], which collocated with the dark appearance in the bright field images [Fig.3 (1^{st} row)]. It may indicate the well-known necrotic core of the spheroid, likely caused by hypoxia and limited nutrient availability [1].

The remaining two spheroids [Highlighted by the yellow boxes in Fig.2] didn't show a clear contrast. It might be because they were out of focus and/or out of the field of view. The out-of-focus issue can be attributed to the variations in the culture medium volume among the wells. On the other hand, the out of the field of view issue might be attributed to the slight shift in the spheroid location. Namely, the spheroid was not exactly located at the centre of the well. To overcome these limitations, further extensions of the proposed ASTS system are required, as discussed in the Discussion section.

4. DISCUSSION

4.1. Further extensions of the current system

As discussed in the result section, out of the 15 spheroids imaged, two spheroids were out of focus and/or out of the field of view. Those spheroids were likely in different depths and were relocated from the centre position of the well. The intra-well variations of the culture medium amount lead to a slight change in the focus position among the wells. To address this limitation, a precise vertical control of the OCT probe by integrating an automated Z-axis translation stage into the XY ASTS system is going to be implemented in the near future. On the other hand, for more accurate lateral positioning of the spheroid, real-time NN-based segmentation of the spheroid is going to be performed. Based on this segmentation, the spheroid central coordinates are going to be determined and fed to the XY stage control to position the stage not at the centre of the well (current implementation), but at the centre of the spheroid. Additionally, combining the current microscope with the NN-based high-speed DOCT imaging (requires only 4 repeated frames at each location) developed by our group [6] will significantly increase the speed of the proposed system and enable scanning 96 wells in approximately 15 minutes.

4.2. Importance of the proposed system.

The automated DOCT microscope described, along with the future developments outlined in Section 4.1, is intended to serve as a fully automated platform for high-throughput imaging of in vitro cultures. This system holds promise as a valuable tool for anti-cancer drug screening. Its automatic targeting capability enables researchers to perform time-course imaging of tumor spheroids with high temporal resolution (i.e., shorter intervals between successive measurements), facilitating fine analysis of spheroid-drug interactions over time.

5. CONCLUSION

We demonstrated an automated sample targeting system (ASTS) and integrated it with a dynamic OCT microscope for high-throughput, label-free imaging of tumor spheroids. The integration of an XY motorized stage with synchronized OCT acquisition via TCP communication enabled fully automated imaging of spheroids within a 96-well plate. A set of 15 spheroids in a 96-well plate was successfully imaged. Among them, only two spheroids appeared to be out of focus and/or FOV. These limitations are going to be addressed by integrating an additional depth-axis (Z-axis) stage for tuning the focus position and establishing an image-based segmentation method, which will enable fine 3D positioning of the sample within the FOV. The proposed system might be a useful tool for high throughput spheroid based anti-cancer drug screening.

6. REFERENCES

[1] I. A. El-Sadek *et.al*., Biomed. Opt. Express **12**, 6844–6862 (2021) **[2]** S. Pi *et.al*., Opt Lett **49**, 4481–4484 (2024) **[3]** V. Lob *et.al*., Med Bio Eng Comput **45**, 1023–1028 (2007) **[4]** T. Geisler *et.al*., IEEE Trans. Automat. Sci. Eng. **3**, 169–176 (2006). **[5]** R. Morishita *et.al*., Biomed. Opt. Express **14**, 2333 (2023) **[6]** Y. Liu *et.al*., Biomed. Opt. Express **15**, 3216 (2024).